The level and compartmentalization of phosphatidate phosphatase-1 (lipin-1) control the assembly and secretion of hepatic VLDL[S]

Maroun Bou Khalil,* Meenakshi Sundaram,* Hong-Yu Zhang,* Philip H. Links,* Jennifer F. Raven,* Boripont Manmontri,† Meltem Sariahmetoglu,† Khai Tran,* Karen Reue,§ David N. Brindley,† and Zemin Yao[1,*]

Department of Biochemistry, Microbiology, and Immunology,* University of Ottawa, Ottawa, Ontario K1H 8M5, Canada; Signal Transduction Research Group, Department of Biochemistry,† University of Alberta, Edmonton, Alberta T6G 2S2, Canada; and Departments of Human Genetics and Medicine,§ David Geffen School of Medicine, University of California, Los Angeles, CA 90095

Abstract Phosphatidate phosphatase-1 (PAP-1) converts phosphatidate to diacylglycerol and plays a key role in the biosynthesis of phospholipids and triacylglycerol (TAG). PAP-1 activity is encoded by members of the lipin family, including lipin-1 (1α and 1β), -2, and -3. We determined the effect of lipin-1 expression on the assembly and secretion of very low density lipoproteins (VLDL) using McA-RH7777 cells. Expression of lipin-1α or -1β increased the synthesis and secretion of [^{3}H]glycerol-labeled lipids under either basal- or oleate-supplemented conditions. In the presence of oleate, the increased TAG secretion was mainly associated with $VLDL_1$ ($S_f > 100$) and $VLDL_2$ (S_f 20–100). Expression of lipin-1α or -1β increased secretion efficiency and decreased intracellular degradation of [^{35}S]apolipoprotein B-100 (apoB100). Knockdown of lipin-1 using specific short interfering RNA decreased secretion of [^{3}H]glycerolipids and [^{35}S]apoB100 even though total PAP-1 activity was not decreased, owing to the presence of lipin-2 and -3 in the cells. Deletion of the nuclear localization signal sequences within lipin-1α not only abolished nuclear localization but also resulted in impaired association with microsomal membranes. Cells expressing the cytosolic lipin-1α mutant failed to promote [^{35}S]apoB100 synthesis or secretion, and showed compromised stimulation in [^{3}H]TAG synthesis and secretion. Thus, alteration in hepatic expression of lipin-1 and its compartmentalization control VLDL assembly/secretion.—Bou Khalil, M., M. Sundaram, H-Y. Zhang, P. H. Links, J. F. Raven, B. Manmontri, M. Sariahmetoglu, K. Tran, K. Reue, D. N. Brindley, and Z. Yao. **The level and compartmentalization of phosphatidate phosphatase-1 (lipin-1) control the assembly and secretion of hepatic VLDL. *J. Lipid Res.* 2009.** 50: **47–58.**

Supplementary key words fatty liver dystrophy • hepatosteatosis • triacylglycerol • hypertriglyceridemia • diabetes • dexamethasone • insulin

The major lipoproteins carrying triacylglycerol (TAG) in fasted human plasma are VLDL that are synthesized by the liver. Formation of hepatic VLDL requires the active synthesis of various lipid constituents (e.g., TAG, cholesterol, cholesteryl esters, and phospholipids) that are assembled together with the large, hydrophobic apolipoprotein B100 (apoB100) (1–3), and the assembly process is initiated during or immediately after translation and translocation of apoB100 across the endoplasmic reticulum (ER) membranes (4). The microsomal triglyceride transfer protein (MTP), encoded by the abetalipoprotenemia gene *mttp*, is essential for VLDL assembly and secretion (5–7), promoting TAG partitioning into the microsomes (8–10). The TAG utilized for the assembly process is derived from de novo glycerolipid biosynthesis and also from hydrolysis/re-esterification of preexisting TAG (11) or phospholipids (12, 13). A key enzyme involved in the de novo biosynthesis of TAG and phospholipids is phosphatidate phosphatase-1 (PAP-1), which converts of phosphatidate (PA) to diacylglycerol (DAG) (14, 15). The resulting DAG serves as substrate for the synthesis of TAG as well as phosphatidylcholine (PC) and phosphatidylethanolamine (PE).

This work was supported by Canadian Institutes of Health Research (CIHR) Grant MT-15486 to Z.Y., and grant MOP 81137 to D.N.B. Z.Y. is a Career Investigator of the Heart and Stroke Foundation of Ontario, and D.N.B. is a recipient of a Medical Scientist Award from the Alberta Heritage Foundation for Medical Research.

Manuscript received 25 April 2008 and in revised form 11 August 2008 and in re-revised form 25 August 2008.

Published, JLR Papers in Press, September 3, 2008.
DOI 10.1194/jlr.M800204-JLR200

Abbreviations: apo, apolipoprotein; DAG, diacylglycerol; ER, endoplasmic reticulum; MTP, microsomal triglyceride transfer protein; NLS, nuclear localization signal; PA, phosphatidate; PAP, phosphatidate phosphatase; PC, phosphatidylcholine; PE, phosphatidylethanolamine; PGC-1α, PPAR coactivator protein-1α; PPARα, peroxisome proliferator-activated receptor-α; siRNA, short interfering RNA; TAG, triacylglycerol.

[1] To whom correspondence should be addressed.
e-mail: zyao@uottawa.ca

[S] The online version of this article (available at http://www.jlr.org) contains supplementary data in the form of two tables.

There are two classes of enzymes that convert PA to DAG in the liver, namely PAP-1 and PAP-2. The PAP-1 activity is specific toward PA and is Mg^{2+}-dependent, and can be inhibited by *N*-ethylmaleimide (15–18). The PAP-2 enzymes degrade a variety of bioactive lipid phosphates, and their activity is *N*-ethylmaleimide-insensitive and Mg^{2+}-independent. In hepatic cells, PAP-1 activity is increased by glucocorticoids, an effect that is synergized by glucagon through cAMP formation and antagonized by insulin (19, 20). Thus, increased PAP-1 activity under stress or other aberrant metabolic conditions (such as starvation, diabetes, and post-alcohol consumption) augments the capacity to sequester an increased FA supply to the liver as TAG (14).

Mammalian PAP-1 is encoded by the lipin gene family, which consists of lipin-1, -2, and -3 (18, 21). The *Lpin1* gene gives rise to two alternative splicing isoforms, lipin-1α and -1β (22). All of these lipins possess PAP-1 activity specific toward PA (18). In mice, lipin-1 is expressed at high levels in adipose tissue, heart, and skeletal muscle, where it is the sole PAP-1 enzyme, and at moderate levels in kidney, lung, brain, and liver (18, 21). In mature 3T3-L1 adipocytes, the two lipin-1 splicing isoforms exhibit different subcellular localization, with lipin-1α being primarily nuclear and lipin-1β cytoplasmic (22). This subcellular localization of lipin-1 appears to influence its function; reconstitution of lipin-1-deficient cells with lipin-1α induces adipogenic gene expression, whereas lipin-1β promotes gene expression of enzymes involved in lipid synthesis (22).

The role of lipin-1 in adipogenic gene expression and TAG biosynthesis in adipose tissue has been documented (22–24). Mutations in the mouse *Lpin1* gene prevent normal adipose tissue development, and result in lipodystrophy (21, 25–27). Transgenic mice expressing lipin-1 specifically in adipocytes have enhanced TAG storage and become obese (23). Lipin-1 also promotes hepatic TAG storage and FA oxidation through transcriptional regulation of the peroxisome proliferator-activated receptor-α (PPARα) and PPAR coactivator protein-1α (PGC-1α) complex (28). Lipin-1 deficiency in the fatty liver dystrophy (*fld*) mouse strain does not preclude hepatic TAG synthesis or secretion during the neonatal period when the animals consume a high-fat diet (29). Rather, PAP-1 activity in *fld* mice is normal, owing to the presence of lipin-2 and probably increased expression of lipin-3 (18).

We have previously shown that TAG synthesis, apoB synthesis and stability, and VLDL secretion in primary rat hepatocytes were all increased by the glucocorticoid dexamethasone, whereas insulin counteracted these effects (30–32). On the basis of recent discoveries showing that *a*) the expression of lipin-1, but not lipin-2 or -3, can be upregulated by glucocorticoids and suppressed by insulin in mouse and rat hepatocytes (33), and *b*) the promoter region of *Lpin1* contains a functional glucocorticoid response element (34), we postulated that lipin-1 is the link between glucocorticoid treatment and enhanced hepatic VLDL secretion. Upregulation of lipin-1 may provide a mechanism for converting excess FAs, derived from lipolysis in adipose tissue in starvation, diabetes, and other conditions of metabolic stress, into TAGs that are secreted as VLDL or stored as lipid droplets (14, 35). In the present study, we tested the effect of alterations in hepatic lipin-1 expression on VLDL assembly and secretion using gain- and loss-of-function approaches for lipin-1α and -1β, as well as for a mutant form of lipin-1α in which the nuclear localization signal (NLS) sequences were deleted. Results presented herein provide strong evidence that the level and compartmentalization of lipin-1 exert a major impact on VLDL assembly and secretion.

METHODS

Materials

Cell culture media and reagents, mouse anti-V5 monoclonal antibody, goat anti-mouse IgG conjugated with Alexa Fluor 488, goat anti-rabbit IgG conjugated with Alexa Fluor 599, and SlowFade Light AntiFade were purchased from Invitrogen (Burlington, ON). DNA restriction and modification enzymes were obtained from New England Biolabs (Pickering, ON). Protein A-Sepharose™ CL-4B beads, [^{35}S]methionine/cysteine (1,000 Ci/mmol), and HRP-linked anti-mouse IgG antibody were obtained from Amersham Biosciences (Baie d'Urfe, PQ). (2-^{3}H]glycerol (9.6 Ci/mmol) was obtained from Amersham (Piscataway, NJ). Protease inhibitor cocktail (EDTA-free) and chemiluminescent substrates were purchased from Roche Diagnostics (Laval, PQ). Lipid standards were obtained from Avanti Polar Lipids (Alabaster, AL). Antibodies against apoE, lamin A, β-actin, and calnexin were obtained from BioDesign (Saco, ME), Abcam (Hornby, ON), Ambion (Austin, TX), and Stressgen (Ann Arbor, MI), respectively. Polyclonal anti-lipin-1 antiserum against the synthetic polypeptide SKTDSPSRKKDKRSRHLGADG (36) and antiserum against rat VLDL were produced in our laboratory.

Mouse lipin-1 expression plasmids and transfection

The coding sequences of lipin-1α, -1β (22), and ΔNLS (a variant of lipin-1α that lacked the NLS sequence KKRRKRRRK) were originally prepared in the pcDNA3.1/V5-His-TOPO expression system. The coding sequences for lipin-1α and -1β were excised by digestion with *Kpn*I and *Pme*I and inserted into the pCMV5 vector that had been digested with *Kpn*I and *Sma*I. The resulting pCMV5-based expression plasmids were transfected into McA-RH7777 cells by the calcium phosphate precipitation method (37). All analyses were performed 48 h posttransfection.

Lipin-1 knockdown

Double-stranded ON-TARGETplus SMARTpool® short interfering RNAs (siRNAs) (see supplementary Table I) specific for rat lipin-1 were obtained from Dharmacon, Inc. (Lafayette, CO). McA-RH7777 cells (50% confluence) were cultured in DMEM containing 20% FBS, and transfected with 80 pmol lipin-1 siRNA (100 nM final concentration) using different concentrations (0.025, 0.05, or 0.075 μg/μl) of Lipofectamine™ 2000 (Invitrogen), according to the manufacturer's instructions. The highest lipin-1 knockdown was observed at 0.075 μg/μl of Lipofectamine; this concentration was used for all subsequent metabolic labeling experiments and for gene expression analyses by real-time RT-PCR. The transfection medium was replaced with DMEM containing 20% FBS 4.5 h posttransfection. For each experiment, controls for lipin-1 knockdown were performed with functional nontargeting control siRNA (Dharmacon), which can silence firefly luciferase, or with Lipofectamine™ 2000 alone. Cells were harvested 48 h after transfection and subjected to

immunoblot analysis (for lipin-1) or used for the metabolic labeling experiments described below.

Analysis of lipin-1 expression

Cell lysates of equal amounts of proteins were resolved by denaturing SDS-PAGE (8% gel), and transferred onto nitrocellulose membranes. Recombinant lipin-1 variants were detected using mouse anti-V5 antibody. In parallel experiments, cells were labeled with [^{35}S]methionine/cysteine (75 μCi/dish) for 4 h in media containing 20% FBS and 0.4 mM oleate. Cell-associated lipin-1 was recovered by immunoprecipitation using polyclonal anti-lipin-1 antiserum, and subjected to denaturing SDS-PAGE (8% gel) and autoradiography.

PAP-1 assay

The PAP-1-specific activity in lipin-1-transfected McA-RH7777 cells and primary rat hepatocytes was determined according to protocols described previously (33).

Immunofluorescence microscopy

Cells cultured on fibronectin-coated coverslips were incubated in DMEM ± 0.4 mM oleate for 2 h at 37°C. Cells were then fixed with 4% paraformaldehyde for 30 min, and then permeabilized with 0.1% Triton X-100 in PBS for 5 min at room temperature. The cells were blocked with 10% FBS (in PBS) for 1 h, rinsed, and incubated with mouse anti-V5 monoclonal antibody (5 μg/ml) plus rabbit anti-lamin A polyclonal antibody (0.1 μg/ml) for 1 h. After rinsing with PBS, cells were stained with goat anti-mouse IgG conjugated with Alexa Fluor 488 and goat anti-rabbit IgG conjugated with Alexa Fluor 599. The coverslips were mounted onto glass slides using SlowFade Light AntiFade. Confocal images were captured using a 100× NA1.4 oil objective on an Olympus IX81 inverted microscope with appropriate lasers (488 nm argon/krypton laser for Alexa 488, and the 543 nm green helium-neon laser for Alexa 599).

Subcellular fractionation

Subcellular fractionation was performed as described previously (9). Briefly, lipin-1 expressing cells (8–10 100 mm dishes) were homogenized by passing 20 times through a ball-bearing homogenizer. Cell homogenates were centrifuged (12,000 *g*, 10 min, 4°C) to obtain nuclear membranes (pellet) and the post-nuclear supernatant, which was transferred to a quick-seal centrifuge tube and centrifuged using a Beckman TLA-100.4 rotor (174,000 *g*, 30 min, 4°C) to obtain cytosol (supernatant) and microsomes (pellet). Aliquots of the fractionated samples were subjected to denaturing SDS-PAGE and immunoblot analysis for lipin-1. Antibodies against lamin, calnexin, and actin were used to probe for nucleus, microsomes, and cytosol, respectively.

Metabolic labeling of lipids

Cells were labeled with [^{3}H]glycerol (4 μCi/ml, 2 ml/dish) in DMEM containing 20% FBS ± oleate (0 to 0.4 mM) for 1, 2, or 4 h. Total lipids were extracted from cells and media, respectively, and separated by TLC as described previously (38). The radioactivity associated with [^{3}H]TAG, -PC, -PE and -DAG was quantified by scintillation counting.

Metabolic labeling of proteins

Cells were labeled with [^{35}S]methionine/cysteine (75 μCi/ml) for 4 h in methionine/cysteine-free DMEM containing 20% FBS ± 0.4 mM oleate. At the end of labeling, the media and cells were collected, and the ^{35}S-labeled apoB100, apoE, and lipin-1 were respectively recovered by immunoprecipitation. Proteins were resolved by denaturing SDS-PAGE (5, 8, and 12% gels for apoB100, lipin-1, and apoE, respectively). Radioactivity associated with these proteins was quantified by scintillation counting (9).

Cumulative rate floatation of secreted lipoproteins

Cells were labeled with [^{3}H]glycerol or [^{35}S]methionine/cysteine as described above. The medium was collected, and the secreted lipoproteins were separated by cumulative rate floatation ultracentrifugation to separate $VLDL_1$ and $VLDL_2$ from the other lipoproteins (9). Lipids were extracted from each lipoprotein fraction and resolved by TLC. The [^{35}S]apoB100 was recovered from each lipoprotein fraction by immunoprecipitation and resolved by denaturing SDS-PAGE as described above.

Pulse-chase analysis of apoB100 and apoE

Cells were pulse-labeled with [^{35}S]methionine/cysteine (75 μCi/ml) for 30 min. The media were removed and replaced with chase media (DMEM containing 20% FBS and 0.4 mM oleate) for up to 4 h. At the end of chase, [^{35}S]apoB100 and -apoE were recovered from media and cells, respectively, by immunoprecipitation, and subjected to denaturing SDS-PAGE and scintillation counting as described previously (9).

MTP activity assay

Lipin-1 expressing cells were suspended in hypotonic buffer (1 mM Tris-HCl, pH 7.4, 1 mM $MgCl_2$, and 1 mM EGTA) containing protease cocktail inhibitors, and homogenized using a Polytron homogenizer. After centrifugation using a Beckman microcentrifuge at 10,000 rpm, 4°C for 30 min, the supernatants were used for MTP activity assay (with 25 μg protein per assay) as described previously (39, 40).

Quantification of RNA by real-time RT-PCR

Isolation of RNA from cells, reverse transcription, and relative mRNA concentration determination by real-time RT-PCR were performed according to previously described protocols using cyclophilin A as control (33). The RT-PCR primer sequences for genes of interest are listed in supplementary Table II.

Statistical analysis

Values are expressed as means ± SE. The significance of differences among control and lipin-1-expressing cells was analyzed using Student's *t*-test, two-sample equal variance. $P < 0.05$ was considered significant.

Other assays

Protein concentrations in the cells were quantified by the Bradford method (41).

RESULTS

Lipin-1 expression level governs glycerolipid synthesis and secretion

Transfection of lipin-1α or -1β plasmids into McA-RH7777 cells resulted in expression of the respective lipin-1 isoforms, which were readily detectable in cell lysate with the anti-V5 antibody (**Fig. 1A**, left panel). Metabolic labeling followed by immunoprecipitation using anti-lipin-1 antibody also detected the recombinant protein (Fig. 1A, right panel). Determination of PAP-1 activity using cell lysates showed increased PAP-1 activity following lipin-1 expression (Fig. 1B). Confocal microscopy of dual immunofluorescent staining

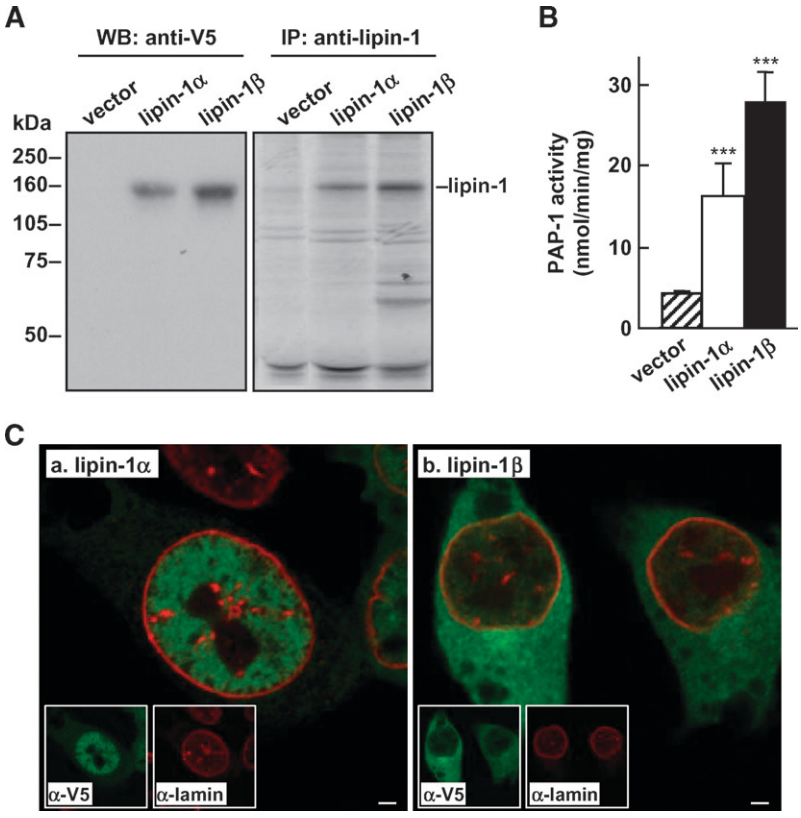

Fig. 1. Transient expression of lipin-1. McA-RH7777 cells were transfected with 5 μg of lipin-1α, lipin-1β, or pCMV5 vector for 48 h. A: Left panel, immunoblots of recombinant lipin-1. Cells were incubated with media containing 20% FBS and 0.4 mM oleate for 4 h, and full cell lysate was subjected to SDS-PAGE and immunoblotting using anti-V5 monoclonal antibody for lipin-1. Right panel, fluorograms of [^{35}S]lipin-1 immunoprecipitated from [^{35}S]methionine-labeled cells using polyclonal anti-lipin-1 antiserum. B: Phosphatidate phosphatase 1 (PAP-1) activity. Cells were incubated with media containing 20% FBS and 0.4 mM oleate for 4 h. Cells were lysed, and the total cell lysate was used to measure PAP-1 activity [determined by the conversion of diacylglycerol (DAG) from [^{3}H]palmitate-labeled phosphatidate]. ***$P < 0.001$ (Student's *t*-test of lipin vs. control). Error bars indicate ± SD (n = 3). C: Representative double immunofluorescent microscopic images of lipin-1α- (panel a) or -1β- (panel b) expressing cells. Images of lipin-1 (green) or lamin (red) staining are shown in insets. Scale bar = 2 μm.

of lamin (nuclear membrane marker) and lipin-1 confirmed that lipin-1α was present predominantly in the nucleus (Fig. 1C, panel a), and lipin-1β in the cytoplasm (panel b). The transfection efficiency of lipin-1 plasmids in these cells was ≤20% as determined by immunofluorescent microscopy.

The respective contribution of lipin-1α and -1β to glycerolipid synthesis and secretion was determined by metabolic labeling experiments under lipid-poor (i.e., no serum, no oleate) or lipid-rich (i.e., supplemented with serum and/or oleate) conditions. Increased incorporation of [^{3}H]glycerol into cell-associated and medium [^{3}H]TAG (and [^{3}H]PC as well) under lipid-poor conditions was observed in both lipin-1α and -1β cells (**Fig. 2A**). Supplementation of oleate into the serum-free media stimulated the incorporation of [^{3}H]glycerol into cell-associated TAG (Fig. 2B).(Note different scales of *y* axis for left panel in Fig. 2A, B.) Under oleate supplement conditions, the rate of [^{3}H]TAG secretion from lipin-1α and -1β cells was markedly increased as compared with vector-transfected controls (Fig. 2B, panel b). Likewise, incorporation of [^{3}H]glycerol into secreted PC, PE, and DAG was also increased from lipin-1α and -1β cells (Fig. 2B, panel b). When metabolic labeling experiments were performed in the presence of serum, an increase in cell-associated and medium [^{3}H]lipids was also observed in lipin-1-expressing cells (Fig. 2C), and oleate supplementation further increased their rate of synthesis and secretion (Fig. 2D). The increased secretion rate of [^{3}H]TAG was positively correlated with the oleate dose (ranging from 0.1 to 0.4 mM; data not shown). Under oleate supplement conditions, the rate of [^{3}H]TAG and [^{3}H]PC secretion from lipin-1α and -1β cells was significantly higher than that from control cells (Fig. 2B, D).

The requirement of lipin-1 for glycerolipid synthesis and secretion was further determined using a loss-of-function approach. Transfection of McA-RH7777 cells with lipin-1-specific siRNA resulted in ∼55% decrease in lipin-1 protein (**Fig. 3A**) and similar decrease in the relative mRNA concentration of lipin-1 (with respect to cyclophilin A) (Fig. 3B). The relative mRNA concentrations of lipin-2 or -3 were not changed significantly by the lipin-1 siRNA treatment (Fig. 3B). The primer efficiencies for lipin-1, -2, and -3 were 1.99, 1.90, and 2.0, respectively, during real-time RT-PCR reactions, and the corresponding cycles required to detect lipin-1, -2, and -3 were 26, 22, and 24. The higher number of threshold cycles required for lipin-1 indicated that lipin-1 may be the least-abundant lipin in McA-RH7777 cells. The lipin-2 or -3 protein levels were not determined, owing to the lack of suitable specific antibodies. The PAP-1 assay showed that lipin-1 siRNA treatment did not decrease the overall PAP-1 activity in the cells (Fig. 3C). This confirms that lipin-1 expression in untreated cells is low compared with that of lipin-2 and -3.

Following lipin-1 knockdown, secretion of [^{3}H]glycerol-labeled TAG, PC, PE, and DAG was reduced by >2-fold as determined by metabolic labeling experiments (Fig. 3D, panel a). The reduced secretion of [^{3}H]glycerolipids was not due to impaired synthesis, as evidenced by nearly equal incorporation of [^{3}H]glycerol into cell-associated TAG

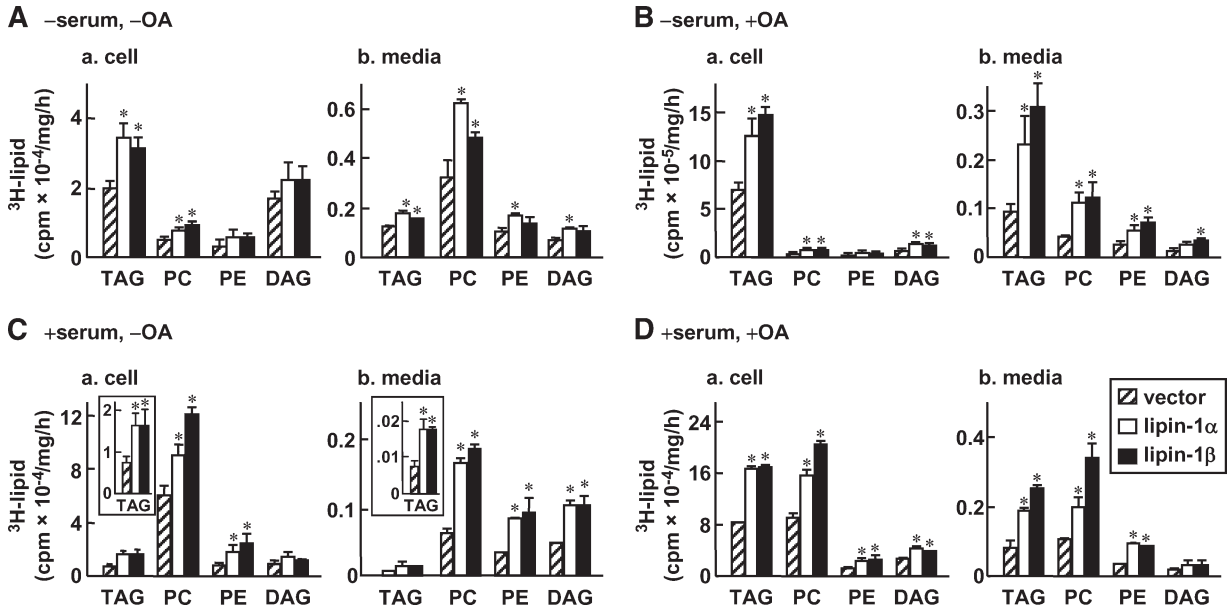

Fig. 2. Expression of lipin-1 stimulates [^{3}H]glycerolipid synthesis and secretion. McA-RH7777 cells were transiently transfected with lipin-1α or -1β as described in the legend of Fig. 1. Cells were labeled with [^{3}H]glycerol (4 μCi/ml) for 1, 2, and 4 h in lipid-poor media (A), in media supplemented with 0.4 mM oleate (B), in media supplemented with 20% FBS (C), or in media supplemented with 20% FBS and 0.4 mM oleate (D). The ^{3}H-lipids were extracted from the cells and media, respectively, at each time point, resolved by TLC, and quantified by scintillation counting. Data are presented as radioactivity counts associated with cell or media per milligram cell protein per hour. Insets in panel C show [^{3}H]TAG in expanded *y* axis. TAG, triacylglycerol; PC, phosphatidylcholine; PE, phosphatidylethanolamine. $*P < 0.05$ (Student's *t*-test of lipin vs. control). Error bars indicate ± SD (n = 3).

between control and lipin-1 siRNA-treated cells (Fig. 3D, panel b). This result is compatible with the lack of an effect of lipin-1 knockdown on total PAP-1 activity, which is contributed mainly by lipin-2 and -3. The observed effect of the knockdown on [^{3}H]glycerolipid secretion points to a specific role of lipin-1 in this process.

The medium lipoproteins secreted from cells cultured under lipid-rich conditions (i.e., + serum and + oleate)

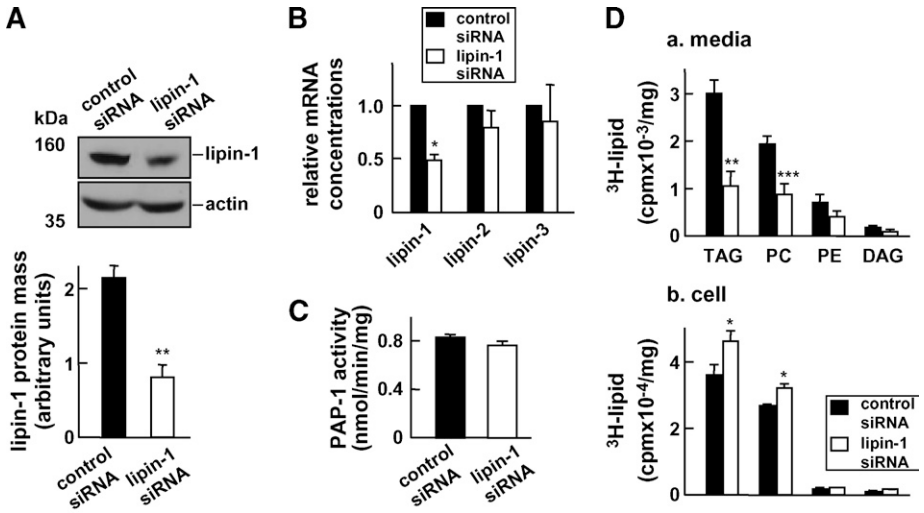

Fig. 3. Lipin-1 knockdown. A: McA-RH7777 cells (50% confluent) were incubated with 80 pmol lipin-1 or control siRNA for 48 h in media supplemented with 20% FBS and 0.4 mM oleate, as described in the Methods section. Endogenous lipin-1 after short interfering RNA (siRNA) treatment was detected by immunoblotting (top panel) as described in the legend of Fig. 1A. The intensity of the lipin bands was semi-quantified by scanning densitometry (bottom panel). B: The relative mRNA concentrations of lipin-1, -2, and -3 (with respect to cyclophilin A) were quantified by real-time RT-PCR. C: PAP-1 activity in control and lipin-1 knockdown cells was determined as in the legend to Fig. 1B. D: Metabolic labeling of medium (panel a) and cell (panel b) glycerolipids with [^{3}H]glycerol as described in Fig. 2D. $*P < 0.05$; $**P < 0.01$; $***P < 0.001$ (Student's *t*-test of lipin vs. control). Error bars indicate ± SD (n = 3).

were fractionated by ultracentrifugation to determine the association of [^{3}H]glycerolipids with various lipoproteins. The increased [^{3}H]TAG secretion from lipin-1α and -1β cells was predominately associated with $VLDL_1$ ($S_f > 100$) and/or $VLDL_2$ (S_f 20–100) (**Fig. 4A**). Although the secreted [^{3}H]PC from lipin-1-expressing cells was found in both VLDLs and HDLs, the significant increase in [^{3}H]PC secretion was associated with VLDL (Fig. 4B). The secretion of [^{3}H]PE in association with lipoproteins was not affected significantly by lipin expression (Fig. 4C), whereas secretion of [^{3}H]DAG in VLDLs was increased, although it did not reach statistical significance (Fig. 4D). These results provide the first indication that de novo synthesis of glycerolipids and their secretion as VLDLs are increased by expression of lipin-1 (regardless of isoform), presumably as a consequence of increased production of DAG in these cells.

Lipin-1 expression level correlates positively with apoB100 synthesis and secretion

Transient expression of lipin-1α or -1β resulted in increased (by 2-fold) incorporation of [^{35}S]methionine into cell-associated (**Fig. 5A**, panel a) and secreted apoB100 (panel b), as compared with controls (i.e., transfected with vector alone). The effect of lipin-1α and -1β was specific to apoB100, because incorporation of [^{35}S]methionine into apoE was unaffected (Fig. 5A, bottom panels). A similar stimulatory effect of lipin-1 expression on [^{35}S]apoB100 secretion was observed when cells were labeled in the absence of oleate (results not shown). Fractionation of medium lipoproteins showed that the increased secretion of [^{35}S]apoB100 from lipin-1α or -1β expressing cells was mainly associated with $VLDL_1$ and $VLDL_2$ (Fig. 5B, C). The combined [^{3}H]TAG (Fig. 4) and [^{35}S]apoB100 (Fig. 5) results indicate that the level of lipin-1α or -1β expression has a major impact on the assembly and secretion of TAG-rich VLDLs in McA-RH7777 cells.

Knockdown of endogenous lipin-1 using siRNA resulted in decreased [^{35}S]apoB100 in the cells (**Fig. 6A**, panel a) and media (panel b) by >2-fold, as compared with controls. Neither the synthesis nor the secretion of apoE was affected following lipin-1 knockdown (Fig. 6A). These results demonstrate that the level of lipin-1 expression in McA-RH7777 cells exerts a strong influence on the synthesis and secretion of apoB100. The relative mRNA concentrations for PGC-1α or PPARα were marginally or unaffected by lipin-1 knockdown (Fig. 6B).

To gain further insight into mechanisms by which the level of lipin-1 expression affects [^{35}S]methionine incorporation into apoB100, we performed pulse (30 min) -chase (up to 4 h) experiments to determine the posttranslational stability and secretion efficiency of newly synthesized apoB100. At the end of 30 min pulse labeling, the incorporation of [^{35}S]methionine into apoB100 in lipin-1α or -1β cells was similar to or slightly higher than that in control cells (**Fig. 7A**, open bars in panel a). The same

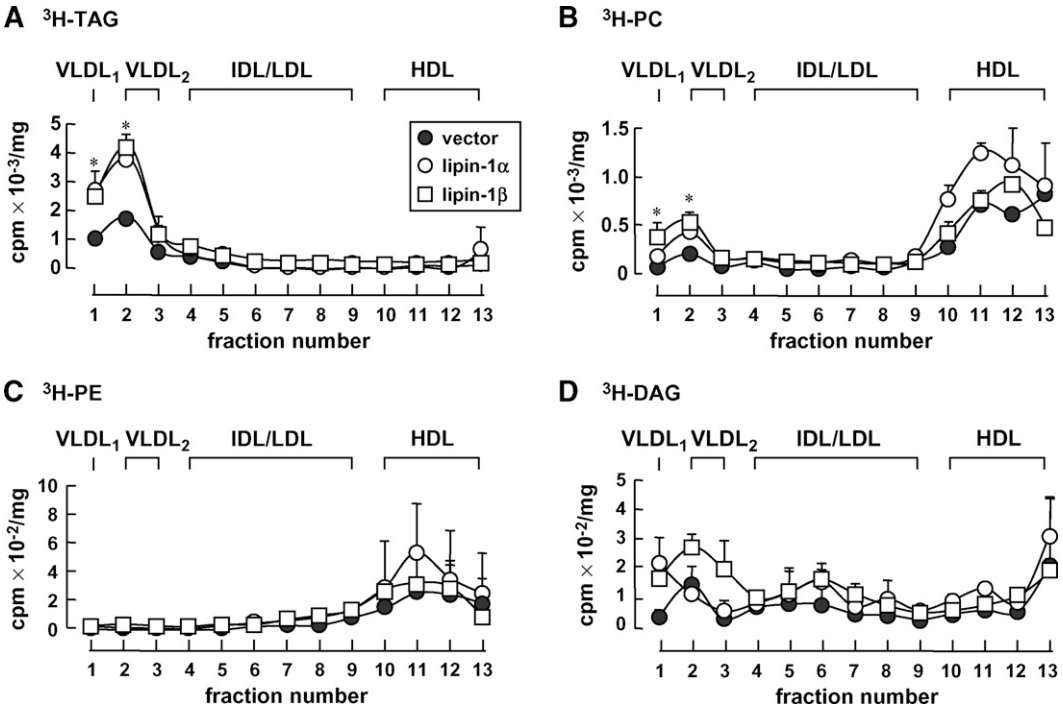

Fig. 4. Increased [^{3}H]TAG association with $VLDL_1$ and $VLDL_2$ secreted from lipin-1 expressing cells. Control or lipin-1-expressing cells were labeled with [^{3}H]glycerol as described in the legend of Fig. 2D. The secreted lipoproteins in the conditioned media were subjected to cumulative rate floatation ultracentrifugation. The ^{3}H-labeled lipids were extracted from each fraction, and TAG (A), PC (B), PE (C), and DAG (D) were resolved by TLC and quantified by scintillation counting. *$P < 0.05$ (Student's *t*-test of lipin vs. control). Error bars indicate ± SD (n = 3).

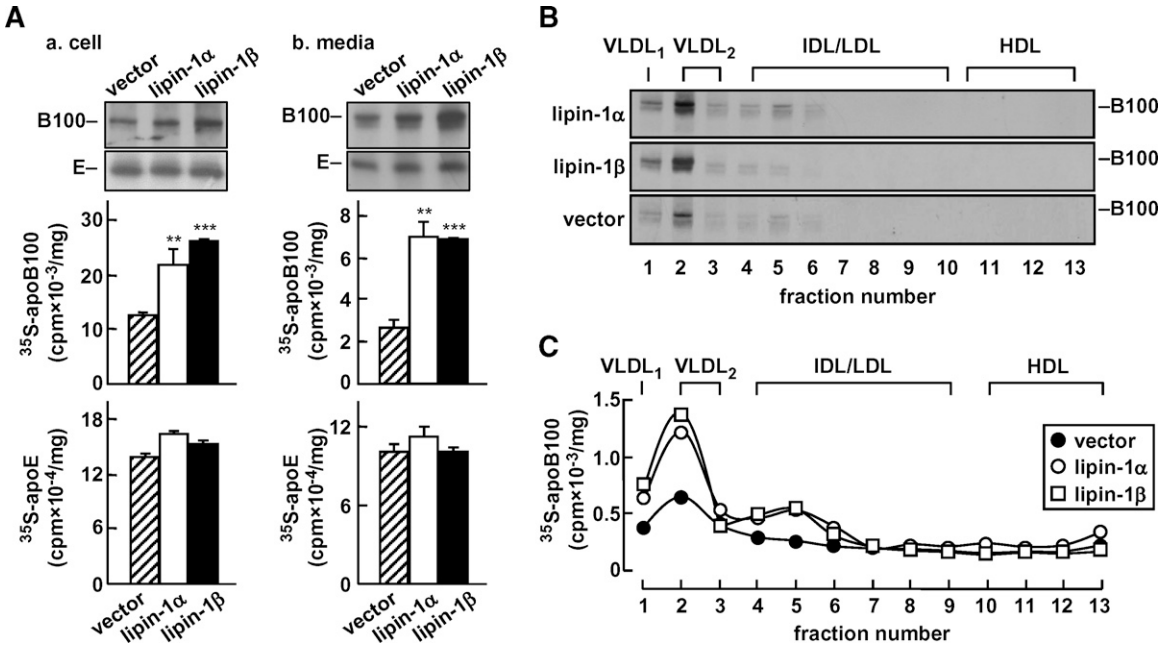

Fig. 5. Expression of lipin-1 stimulates [^{35}S]apolipoprotein B100 (apoB100) secretion as $VLDL_1$ and $VLDL_2$. Control or lipin-1 expressing cells were continuously labeled with [^{35}S]methionine/cysteine (75 μCi/dish) for 4 h in media containing 20% FBS and 0.4 mM oleate. The [^{35}S]apoB100 or -apoE was recovered from cells or media by immunoprecipitation and subjected to SDS-PAGE and fluorography. A: Top, representative fluorograms of [^{35}S]apoB100 and -apoE associated with cells or media. Bottom, radioactivity associated with apoB and apoE. $^{**}P < 0.01$; $^{***}P < 0.001$ (Student's *t*-test of lipin vs. control). Error bars indicate ± SD (n = 3). B: Representative fluorograms of ^{35}S-labeled apoB100 associated with fractionated medium lipoproteins. C: Radioactivity associated with [^{35}S]apoB100 in each lipoprotein fraction was quantified by scintillation counting.

trend was observed when pulse labeling was performed in the presence of the proteasome inhibitor MG132 to block cotranslational apoB100 degradation (Fig. 7A, closed bars in panel a). At the end of the initial 30 min chase, the incorporation of [^{35}S]methionine into apoB100 in lipin-1α and lipin-1β cells was noticeably higher than that in control cells (Fig. 7A, panel b). These results are in agreement with our metabolic labeling studies showing increased apoB100 accumulation in the cells upon lipin-1 expression (Fig. 5A). We next determined the secretion efficiency of apoB100 at 30 min and up to 4 h chase. Secretion efficiency was defined as the percent of newly synthesized apoB100 proteins secreted during chase. Representative fluorograms of [^{35}S]apoB100 in cells and media during

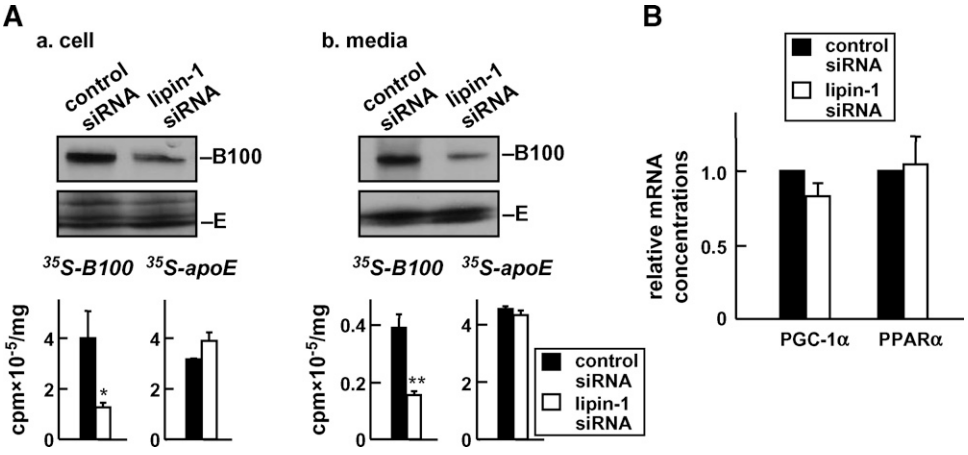

Fig. 6. Synthesis and secretion of [^{35}S]apoB100 in lipin-1 knockdown cells. A: Control or lipin-1 siRNA-treated cells were labeled with [^{35}S]methionine/cysteine as described in the legend of Fig. 5. Top, representative fluorograms of cell-associated (left panel) or secreted (right panel) [^{35}S]apoB100 and -apoE. Bottom, radioactivity associated with apoB and apoE. $^{*}P < 0.05$; $^{**}P < 0.01$ (Student's *t*-test of lipin vs. control). B: Effect of lipin-1 knockdown on the relative concentrations of peroxisome proliferator-activated receptor-α (PPARα) and PPAR coactivator protein-1α (PGC-1α) mRNAs. Error bars indicate ± SD (n = 3).

chase are shown in the top panels of Fig. 7B, C. Quantification of radioactivity associated with [^{35}S]apoB100 showed that the secretion efficiency of apoB100 (particularly between 1 and 2 h chase) was increased from lipin-1α and -1β expressing cells as compared with vector-transfected controls (Fig. 7B, bottom panel). Similarly to what was observed for [^{3}H]TAG secretion (Fig. 2D), lipin-1β exerted a greater effect than lipin-1α on apoB100 secretion efficiency, as demonstrated throughout the entire chase period (Fig. 7B, bottom panel). The cell-associated apoB100 during chase was not affected by lipin-1α or -1β expression (Fig. 7B, middle panel). The kinetics of cell-associated apoE was not affected by lipin-1α or -1β expression, nor was apoE secretion efficiency (data not shown). In experiments where MG132 was included in the pulse-labeling media, the stimulatory effect of lipin-1β on apoB100 secretion was diminished (Fig. 7C, bottom panel). Under these conditions (i.e., blockage of proteasome function during pulse labeling), secretion of apoB100 from vector-transfected control cells was nearly as efficient as that from lipin-1β cells. These results suggest that the increased apoB100 secretion efficiency observed in lipin-1β cells was at least partly attributable to attenuated cotranslational degradation of newly synthesized apoB100. The MG132 treatment had little effect on apoB100 secretion from lipin-1α-expressing cells, and apoB100 secretion efficiency from lipin-1β cells was higher than that from lipin-1α cells under MG132 treatment conditions (Fig. 7C, bottom panel). The MG132 treatment had little effect on cell-associated apoB100 (Fig. 7C, middle panel) or apoE (results not shown). Determination of lipid transfer activity of MTP using cell lysates showed that transient expression of lipin-1α or -1β in McA-RH7777 cells had little effect on MTP (results not shown). These results indicate that expression of lipin-1, especially lipin-1β, confers a stimulatory effect on apoB100 secretion efficiency, presumably through decreasing cotranslational degradation of newly synthesized apoB100.

Deletion of the NLS in lipin-1α reduces the synthesis and secretion of [^{3}H]TAG and [^{35}S]apoB100

Because lipin-1α and -1β differ in their subcellular localization, we considered the possibility that their different effects on apoB100 secretion efficiency (Fig. 7B, C) might be attributable to compartmentalization of lipin-1 isoforms. Thus, we contrasted the function of wild-type lipin-1α in hepatic glycerolipid synthesis with that of a variant that lacked the NLS sequence (ΔNLS). Transfection of the ΔNLS plasmid into McA-RH7777 cells resulted in normal expression of the protein (**Fig. 8A**). As expected, the ΔNLS

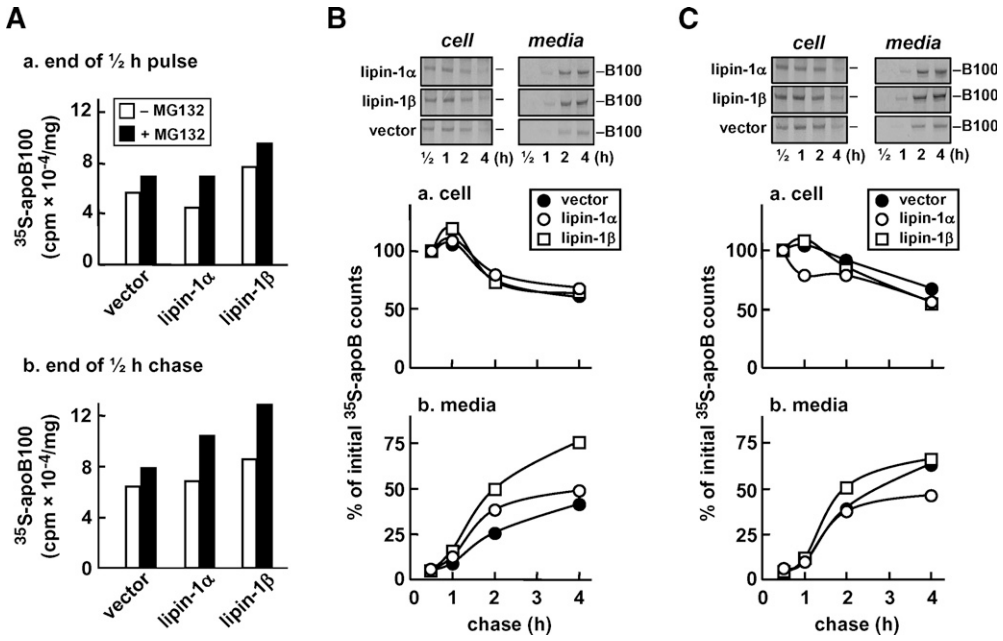

Fig. 7. Pulse-chase analysis of apoB100. Cells were pulse-labeled with [^{35}S]methionine/cysteine (75 μCi/dish) for 30 min in the absence or presence of the proteasomal inhibitor MG132 (25 μM) and "chased" for up to 4 h. Both pulse and chase media contained 20% serum and 0.4 mM oleate. The ^{35}S-labeled apoB100 was recovered from cells and media, respectively, at the indicated times by immunoprecipitation, resolved by SDS-PAGE, and subjected to fluorography. A: Radioactivity counts associated with cell [^{35}S]apoB100 at the end of a 30 min pulse (panel a) and at the end of a 30 min chase (panel b) in the absence (open bars) or presence (closed bars) of MG132. B, C: Top, representative fluorograms of [^{35}S]apoB100 associated with cell or media in the absence (B) or presence (C) of MG132 during chase. Radioactivity associated with apoB100 in cells (panel a) or media (panel b) was quantified, and data are presented as percent of initial counts, which are counts associated with cell [^{35}S]apoB100 at the end of a 30 min chase. The experiment was repeated, and identical results were obtained.

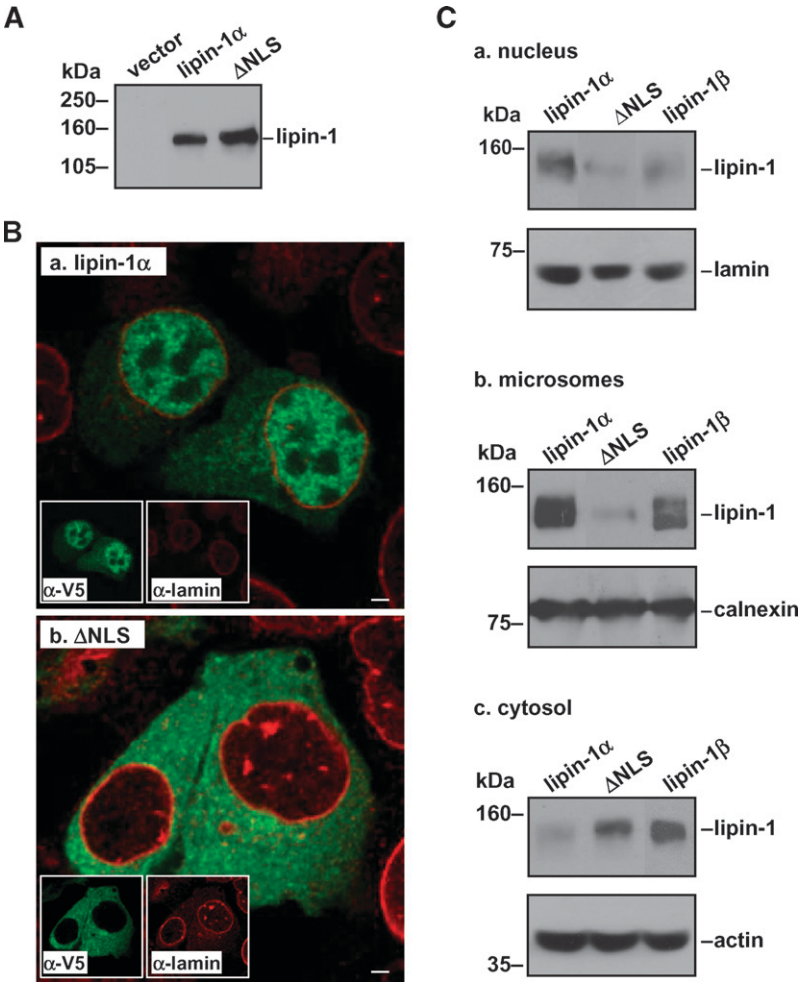

Fig. 8. Expression of the nuclear localization signal deletion (ΔNLS) mutant form of lipin-1α. A: Western blot analysis of the expressed lipin-1α and ΔNLS in transfected cells. The experiment was performed essentially the same as described in the legend of Fig. 1A. B: Representative double immunofluorescent microscopic images of lipin-1α (panel a) or ΔNLS (panel b) expressing cells. Images of lipin-1 (green) or lamin (red) staining are shown in insets. Scale bar = 2 μm. C: Western blots of lipin-1α, ΔNLS, and lipin-1β in the nucleus (panel a), microsomes (panel b), and cytosol (panel c) fractions. Lamin, calnexin, and actin were probed as markers for nucleus, endoplasmic reticulum, and cytosol, respectively.

protein lost its nuclear localization, and appeared predominantly in the cytoplasm (Fig. 8B). Subcellular fractionation experiments confirmed the lack of nuclear localization of the ΔNLS mutant (Fig. 8C, panel a). However, unlike wild-type lipin-1α or -1β, the ΔNLS mutant lost the ability to associate with microsomal membranes (Fig. 8C, panel b) and became mainly cytosolic (panel c). These results suggest that the NLS sequences not only govern nuclear localization but also determine membrane association and physiological function of lipin-1α.

The expression of ΔNLS increased PAP-1 activity to nearly the same extent as the wild-type lipin-1α (**Fig. 9A**). Metabolic labeling experiments showed that cell-associated [^{3}H]TAG and -PC were lower in ΔNLS expressing cells as compared with those expressing the wild-type lipin-1α (Fig. 9B, panel a). Likewise, secretion of [^{3}H]TAG and -PC was also decreased from ΔNLS expressing cells as compared with wild-type lipin-1α (Fig. 9B, panel b). However, as compared with vector-transfected controls, expression of ΔNLS stimulated [^{3}H]glycerolipid synthesis and secretion. Unlike that of the wild-type lipin-1α, expression of ΔNLS failed to stimulate incorporation of [^{35}S]methionine into cell (Fig. 9C, panel a) or secreted (panel b) apoB100. Synthesis or secretion of apoE was not affected by lipin-1α or ΔNLS expression (Fig. 9C). These results indicate that the subcellular localization of lipin-1α indeed has an impact on hepatic lipogenesis and apoB100 synthesis/secretion.

DISCUSSION

Lipin-1 expression is a specific target for differential regulation by glucocorticoids and insulin in the liver, and this has important physiological significance. In primary rat and mouse hepatocytes, dexamethasone treatment stimulates the expression of lipin-1, but not lipin-2 or -3, through a glucocorticoid response element within the *Lpin1* promoter (33, 34). Our present transfection studies with McA-RH7777 cells suggest that although lipin-1, -2, and -3 all encode PAP-1 activity in these cells (Fig. 3), it is lipin-1 that is responsible for the previously observed increase in VLDL secretion upon glucocorticoid treatment (30–32). The observed close relationship between lipin-1 expression (gain- and loss-of-function) and apoB100 synthesis and secretion (Figs. 5A, 6A) underscores the importance of lipid substrate availability in promoting VLDL assembly and decreasing cotranslational degradation of apoB. In accordance with this, overexpression of acyl-CoA:diacylglycerol acyltransferase ($DGAT_1$), the enzyme that catalyzes the final step in the de novo TAG biosyn-

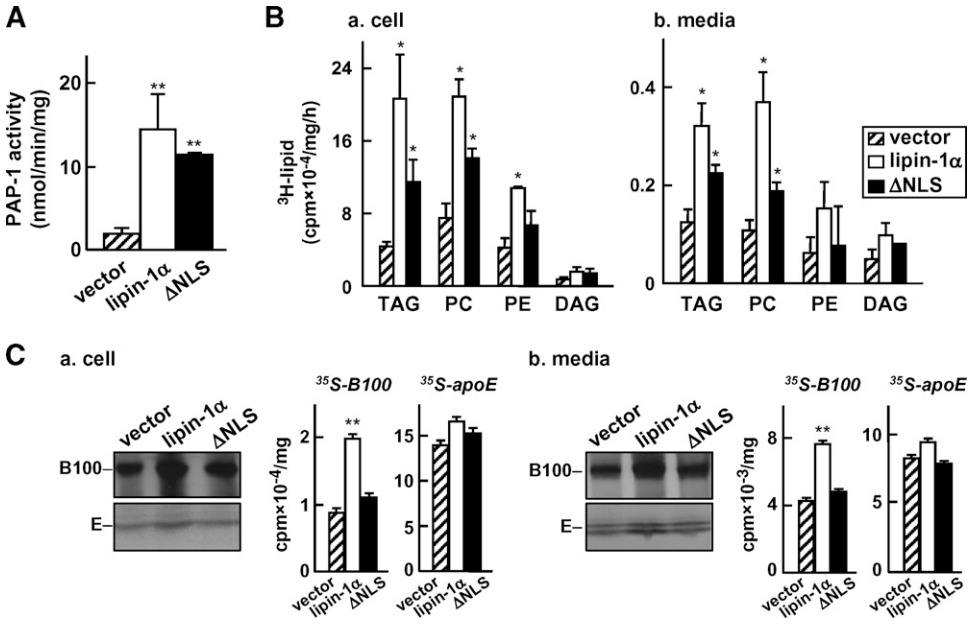

Fig. 9. The ΔNLS mutation compromised the effect of lipin-1α on [^{35}S]apoB100 and [^{3}H]TAG synthesis/secretion. A: PAP-1 activity in control, lipin-1α, and ΔNLS transfected cells. The experiment was performed as described in the legend of Fig. 1B. B: Metabolic labeling of lipids in control, lipin-1α, and ΔNLS transfected cells. The experiment was performed as described in the legend of Fig. 2D. C: Metabolic labeling of apoB and apoE in control, lipin-1α, and ΔNLS transfected cells. The experiment was performed as described in the legend of Fig. 5A. $*P < 0.05$; $**P < 0.01$ (Student's *t*-test of lipin vs. control). Error bars indicate ± SD (n = 3).

thesis pathway, also results in increased hepatic TAG concentrations and VLDL secretion (42, 43). Because lipin-2 and -3 are present in McA-RH7777 cells, simply knocking down lipin-1 did not result in a noticeable decrease in PAP-1 activity (Fig. 3C). This suggests that the three lipin proteins can compensate each other in the total expression of PAP-1 activity (18). However, it is specifically lipin-1 that is responsible for the glucocorticoid-induced increase in PAP-1 activity (33). Despite the lack of changes in total PAP-1 activity following lipin-1 knockdown, [^{3}H]TAG secretion was reduced significantly (Fig. 3D). Therefore, the present work demonstrates that alterations in lipin-1 expression produce parallel changes in VLDL assembly and secretion.

Several lines of evidence reported herein point out that the increased VLDL-apoB100 and VLDL-TAG secretion following lipin-1 expression is not merely a result of a general increase in the lipid availability. Rather, association of lipin-1 with the ER is of particular importance in determining its function in VLDL assembly and secretion. Subcellular fractionation experiments revealed that although lipin-1α and -1β phenotypically exhibited nuclear and cytoplasmic localization, both proteins showed extensive association with the microsomal membranes (Fig. 8C). Close examination of lipin-1α compartmentalization by using the ΔNLS mutant form of lipin-1α revealed that NLS deletion resulted in not only loss of nuclear localization but also loss of microsomal membrane association (Fig. 8C). Moreover, expression of the lipin-1α ΔNLS mutant failed to stimulate [^{35}S]apoB100 or [^{3}H]TAG secretion, even though the mutant retained normal PAP-1 activity (Fig. 9). Thus, a close association of lipin-1, either -1α or -1β, with the ER conceivably governs the lipid substrate availability for VLDL assembly. It has been reported previously that the association of lipin-1 with microsomal membranes can be reduced by insulin treatment (44). Insulin is known to antagonize hepatic VLDL assembly and secretion (31). On the other hand, increased association of lipin-1 with the ER membranes was observed in cells treated with oleate (44), which explains the early observations that translocation of PAP-1 activity from the cytosol to microsomes was promoted by exogenous oleate (45, 46). Altogether, these results suggest strongly that association of lipin-1/PAP-1 with the ER has a major impact on hepatic VLDL assembly and secretion.

The functional significance of lipin-1α association with the nucleus is not immediately clear. It has been reported that the yeast homolog of the mammalian lipin-1, Pah1p/Smp2p (21), is a nuclear protein and a key regulator of phospholipid biosynthetic gene transcription and nuclear/ER membrane growth (47). The cellular functions of Pah1p/Smp2p are dependent upon its PAP-1 activity, which is required for normal nuclear/ER membrane structure (48). Lipin-1 in yeast and mammalian cells has also been shown to associate with chromatin and transcription factors of several genes (28, 47). For instance, mouse lipin-1 interacts directly with PPARα and PGC-1α, and promotes transcriptional regulation of enzymes involved in β-oxidation (28), thus raising the possibility that lipin-1 may serve a dual function in glycerolipid synthesis and transcription regulation. The present studies showed that transient expression

of lipin-1 had little effect on the expression of PGC-1α or PPARα in McA-RH7777 cells (Fig. 6B). Thus, the effect of changing lipin-1 expression on VLDL assembly and secretion in the current cell model system is achieved primarily by regulating hepatic lipogenesis.

Understanding the role that lipin-1 plays in VLDL assembly and secretion has important implications in understanding the mechanisms by which hormonal regulation impacts VLDL production under conditions of starvation, insulin resistance, diabetes, stress, and alcohol intoxication. Under such conditions, increased glucocorticoid production stimulates hepatic PAP-1 (lipin-1) activity and VLDL secretion (30–32), whereas these effects are suppressed by insulin (20, 31, 49). The present work provides evidence that the opposing effects of dexamethasone and insulin on VLDL secretion are mediated through the modulation of lipin-1 expression and its subcellular compartmentalization. This information is important in understanding how the liver maintains the capacity to secrete VLDL in starvation and diabetes, and why hypertriglyceridemia normally accompanies insulin resistance.

The authors thank Drs. Jahangir Iqbal and Mahmood Hussain (SUNY Downstate Medical Center) for performing the MTP activity assay, Michelle Bamji-Mirza, Shumei Zhong, and Jay Dewald for technical assistance, and Dr. Yuwei Wang for critical reading of the manuscript.

REFERENCES

1. Fisher, E. A., and H. N. Ginsberg. 2002. Complexity in the secretory pathway: the assembly and secretion of apolipoprotein B-containing lipoproteins. *J. Biol. Chem.* **277:** 17377–17380.
2. Rustaeus, S., K. Lindberg, P. Stillemark, C. Claesson, L. Asp, T. Larsson, J. Boren, and S. O. Olofsson. 1999. Assembly of very low density lipoprotein: a two-step process of apolipoprotein B core lipidation. *J. Nutr.* **129:** 463S–466S.
3. Olofsson, S. O., L. Asp, and J. Boren. 1999. The assembly and secretion of apolipoprotein B-containing lipoproteins. *Curr. Opin. Lipidol.* **10:** 341–346.
4. Gibbons, G. F., D. Wiggins, A. M. Brown, and A. M. Hebbachi. 2004. Synthesis and function of hepatic very-low-density lipoprotein. *Biochem. Soc. Trans.* **32:** 59–64.
5. Gordon, D. A., J. R. Wetterau, and R. E. Gregg. 1995. Microsomal triglyceride transfer protein: a protein complex required for the assembly of lipoprotein particles. *Trends Cell Biol.* **5:** 317–321.
6. Rustaeus, S., P. Stillemark, K. Lindberg, D. Gordon, and S. O. Olofsson. 1998. The microsomal triglyceride transfer protein catalyzes the post-translational assembly of apolipoprotein B-100 very low density lipoprotein in McA-RH7777 cells. *J. Biol. Chem.* **273:** 5196–5203.
7. Olofsson, S. O., P. Stillemark-Billton, and L. Asp. 2000. Intracellular assembly of VLDL: two major steps in separate cell compartments. *Trends Cardiovasc. Med.* **10:** 338–345.
8. Kulinski, A., S. Rustaeus, and J. E. Vance. 2002. Microsomal triacylglycerol transfer protein is required for lumenal accretion of triacylglycerol not associated with apoB, as well as for apoB lipidation. *J. Biol. Chem.* **277:** 31516–31525.
9. Wang, Y., K. Tran, and Z. Yao. 1999. The activity of microsomal triglyceride transfer protein is essential for accumulation of triglyceride within microsomes in McA-RH7777 cells. A unified model for the assembly of very low density lipoproteins. *J. Biol. Chem.* **274:** 27793–27800.
10. Raabe, M., M. M. Veniant, M. A. Sullivan, C. H. Zlot, J. Bjorkegren, L. B. Nielsen, J. S. Wong, R. L. Hamilton, and S. G. Young. 1999. Analysis of the role of microsomal triglyceride transfer protein in the liver of tissue-specific knockout mice. *J. Clin. Invest.* **103:** 1287–1298.
11. Gilham, D., M. Alam, W. Gao, D. E. Vance, and R. Lehner. 2005. Triacylglycerol hydrolase is localized to the endoplasmic reticulum by an unusual retrieval sequence where it participates in VLDL assembly without utilizing VLDL lipids as substrates. *Mol. Biol. Cell.* **16:** 984–996.
12. Tran, K., F. Sun, Z. Cui, G. Thorne-Tjomsland, C. St Germain, L. R. Lapierre, R. S. McLeod, J. C. Jamieson, and Z. Yao. 2006. Attenuated secretion of very low density lipoproteins from McA-RH7777 cells treated with eicosapentaenoic acid is associated with impaired utilization of triacylglycerol synthesized via phospholipid remodeling. *Biochim. Biophys. Acta.* **1761:** 463–473.
13. Wiggins, D., and G. F. Gibbons. 1996. Origin of hepatic very-low-density lipoprotein triacylglycerol: the contribution of cellular phospholipid. *Biochem. J.* **320:** 673–679.
14. Brindley, D. N. 1988. Phosphatidate Phosphohydrolase: Its Role in Glycerolipid Synthesis. CRC Press, Inc., Boca Raton. 21–77.
15. Carman, G. M., and G. S. Han. 2006. Roles of phosphatidate phosphatase enzymes in lipid metabolism. *Trends Biochem. Sci.* **31:** 694–699.
16. Jamal, Z., A. Martin, A. Gomez-Munoz, and D. N. Brindley. 1991. Plasma membrane fractions from rat liver contain a phosphatidate phosphohydrolase distinct from that in the endoplasmic reticulum and cytosol. *J. Biol. Chem.* **266:** 2988–2996.
17. Brindley, D. N. 2004. Lipid phosphate phosphatases and related proteins: signaling functions in development, cell division, and cancer. *J. Cell. Biochem.* **92:** 900–912.
18. Donkor, J., M. Sariahmetoglu, J. Dewald, D. N. Brindley, and K. Reue. 2007. Three mammalian lipins act as phosphatidate phosphatases with distinct tissue expression patterns. *J. Biol. Chem.* **282:** 3450–3457.
19. Sturton, R. G., S. C. Butterwith, S. L. Burditt, and D. N. Brindley. 1981. Effects of starvation, corticotropin injection and ethanol feeding on the activity and amount of phosphatidate phosphohydrolase in rat liver. *FEBS Lett.* **126:** 297–300.
20. Pittner, R. A., R. Fears, and D. N. Brindley. 1985. Effects of cyclic AMP, glucocorticoids and insulin on the activities of phosphatidate phosphohydrolase, tyrosine aminotransferase and glycerol kinase in isolated rat hepatocytes in relation to the control of triacylglycerol synthesis and gluconeogenesis. *Biochem. J.* **225:** 455–462.
21. Peterfy, M., J. Phan, P. Xu, and K. Reue. 2001. Lipodystrophy in the *fld* mouse results from mutation of a new gene encoding a nuclear protein, lipin. *Nat. Genet.* **27:** 121–124.
22. Peterfy, M., J. Phan, and K. Reue. 2005. Alternatively spliced lipin isoforms exhibit distinct expression pattern, subcellular localization, and role in adipogenesis. *J. Biol. Chem.* **280:** 32883–32889.
23. Phan, J., M. Peterfy, and K. Reue. 2004. Lipin expression preceding peroxisome proliferator-activated receptor-gamma is critical for adipogenesis in vivo and in vitro. *J. Biol. Chem.* **279:** 29558–29564.
24. Phan, J., M. Peterfy, and K. Reue. 2005. Biphasic expression of lipin suggests dual roles in adipocyte development. *Drug News Perspect.* **18:** 5–11.
25. Phan, J., and K. Reue. 2005. Lipin, a lipodystrophy and obesity gene. *Cell Metab.* **1:** 73–83.
26. Reue, K., and M. Peterfy. 2000. Mouse models of lipodystrophy. *Curr. Atheroscler. Rep.* **2:** 390–396.
27. Reue, K., P. Xu, X. P. Wang, and B. G. Slavin. 2000. Adipose tissue deficiency, glucose intolerance, and increased atherosclerosis result from mutation in the mouse fatty liver dystrophy (*fld*) gene. *J. Lipid Res.* **41:** 1067–1076.
28. Finck, B. N., M. C. Gropler, Z. Chen, T. C. Leone, M. A. Croce, T. E. Harris, J. C. Lawrence, Jr., and D. P. Kelly. 2006. Lipin 1 is an inducible amplifier of the hepatic PGC-1alpha/PPARalpha regulatory pathway. *Cell Metab.* **4:** 199–210.
29. Langner, C. A., E. H. Birkenmeier, O. Ben Zeev, M. C. Schotz, H. O. Sweet, M. T. Davisson, and J. I. Gordon. 1989. The fatty liver dystrophy (*fld*) mutation. A new mutant mouse with a developmental abnormality in triglyceride metabolism and associated tissue-specific defects in lipoprotein lipase and hepatic lipase activities. *J. Biol. Chem.* **264:** 7994–8003.
30. Martin-Sanz, P., J. E. Vance, and D. N. Brindley. 1990. Stimulation of apolipoprotein secretion in very-low-density and high-density lipoproteins from cultured rat hepatocytes by dexamethasone. *Biochem. J.* **271:** 575–583.
31. Mangiapane, E. H., and D. N. Brindley. 1986. Effects of dexamethasone and insulin on the synthesis of triacylglycerols and phospha-

tidylcholine and the secretion of very-low-density lipoproteins and lysophosphatidylcholine by monolayer cultures of rat hepatocytes. *Biochem. J.* **233:** 151–160.
32. Wang, C. N., R. S. McLeod, Z. Yao, and D. N. Brindley. 1995. Effects of dexamethasone on the synthesis, degradation, and secretion of apolipoprotein B in cultured rat hepatocytes. *Arterioscler. Thromb. Vasc. Biol.* **15:** 1481–1491.
33. Manmontri, B., M. Sariahmetoglu, J. Donkor, M. B. Khalil, M. Sundaram, Z. Yao, K. Reue, R. Lehner, and D. N. Brindley. 2008. Glucocorticoids and cyclic AMP selectively increase hepatic lipin-1 expression, and insulin acts antagonistically. *J. Lipid Res.* **49:** 1056–1067.
34. Zhang, P., L. O'Loughlin, D. N. Brindley, and K. Reue. 2008. Regulation of lipin-1 gene expression by glucocorticoids during adipogenesis. *J. Lipid Res.* **49:** 1519–1528.
35. Pittner, R. A., R. Fears, and D. N. Brindley. 1985. Interactions of insulin, glucagon and dexamethasone in controlling the activity of glycerol phosphate acyltransferase and the activity and subcellular distribution of phosphatidate phosphohydrolase in cultured rat hepatocytes. *Biochem. J.* **230:** 525–534.
36. Huffman, T. A., I. Mothe-Satney, and J. C. Lawrence, Jr. 2002. Insulin-stimulated phosphorylation of lipin mediated by the mammalian target of rapamycin. *Proc. Natl. Acad. Sci. USA.* **99:** 1047–1052.
37. Chen, C., and H. Okayama. 1987. High-efficiency transformation of mammalian cells by plasmid DNA. *Mol. Cell. Biol.* **7:** 2745–2752.
38. Tran, K., Y. Wang, C. J. DeLong, Z. Cui, and Z. Yao. 2000. The assembly of very low density lipoproteins in rat hepatoma McA-RH7777 cells is inhibited by phospholipase A2 antagonists. *J. Biol. Chem.* **275:** 25023–25030.
39. Athar, H., J. Iqbal, X. C. Jiang, and M. M. Hussain. 2004. A simple, rapid, and sensitive fluorescence assay for microsomal triglyceride transfer protein. *J. Lipid Res.* **45:** 764–772.
40. Rava, P., H. Athar, C. Johnson, and M. M. Hussain. 2005. Transfer of cholesteryl esters and phospholipids as well as net deposition by microsomal triglyceride transfer protein. *J. Lipid Res.* **46:** 1779–1785.
41. Bradford, M. M. 1976. A rapid and sensitive method for the quantitation of microgram quantities of protein utilizing the principle of protein-dye binding. *Anal. Biochem.* **72:** 248–254.
42. Yamazaki, T., E. Sasaki, C. Kakinuma, T. Yano, S. Miura, and O. Ezaki. 2005. Increased very low density lipoprotein secretion and gonadal fat mass in mice overexpressing liver DGAT1. *J. Biol. Chem.* **280:** 21506–21514.
43. Liang, J. J., P. Oelkers, C. Guo, P. C. Chu, J. L. Dixon, H. N. Ginsberg, and S. L. Sturley. 2004. Overexpression of human diacylglycerol acyltransferase 1, acyl-coA:cholesterol acyltransferase 1, or acyl-CoA:cholesterol acyltransferase 2 stimulates secretion of apolipoprotein B-containing lipoproteins in McA-RH7777 cells. *J. Biol. Chem.* **279:** 44938–44944.
44. Harris, T. E., T. A. Huffman, A. Chi, J. Shabanowitz, D. F. Hunt, A. Kumar, and J. C. Lawrence, Jr. 2007. Insulin controls subcellular localization and multisite phosphorylation of the phosphatidic acid phosphatase, lipin 1. *J. Biol. Chem.* **282:** 277–286.
45. Cascales, C., E. H. Mangiapane, and D. N. Brindley. 1984. Oleic acid promotes the activation and translocation of phosphatidate phosphohydrolase from the cytosol to particulate fractions of isolated rat hepatocytes. *Biochem. J.* **219:** 911–916.
46. Martin, A., R. Hopewell, P. Martin-Sanz, J. E. Morgan, and D. N. Brindley. 1986. Relationship between the displacement of phosphatidate phosphohydrolase from the membrane-associated compartment by chlorpromazine and the inhibition of the synthesis of triacylglycerol and phosphatidylcholine in rat hepatocytes. *Biochim. Biophys. Acta.* **876:** 581–591.
47. Santos-Rosa, H., J. Leung, N. Grimsey, S. Peak-Chew, and S. Siniossoglou. 2005. The yeast lipin Smp2 couples phospholipid biosynthesis to nuclear membrane growth. *EMBO J.* **24:** 1931–1941.
48. Han, G. S., S. Siniossoglou, and G. M. Carman. 2007. The cellular functions of the yeast lipin homolog PAH1p are dependent on its phosphatidate phosphatase activity. *J. Biol. Chem.* **282:** 37026–37035.
49. Pittner, R. A., P. Bracken, R. Fears, and D. N. Brindley. 1986. Insulin antagonises the growth hormone-mediated increase in the activity of phosphatidate phosphohydrolase in isolated rat hepatocytes. *FEBS Lett.* **202:** 133–136.